Synchronization and beam forming in an array of repulsively coupled oscillators

N. F. Rulkov,[1,2] L. Tsimring,[1] M. L. Larsen,[2] and M. Gabbay[2]
[1]*Institute for Nonlinear Science, University of California, San Diego, La Jolla, California 92093-0402, USA*
[2]*Information Systems Laboratories, Inc., San Diego, California 92121, USA*
(Received 1 June 2006; published 15 November 2006)

We study the dynamics of an array of Stuart-Landau oscillators with repulsive coupling. Autonomous network with global repulsive coupling settles on one from a continuum of synchronized regimes characterized by zero mean field. Driving this array by an external oscillatory signal produces a nonzero mean field that follows the driving signal even when the oscillators are not locked to the external signal. At sufficiently large amplitude the external signal synchronizes the oscillators and locks the phases of the array oscillations. Application of this system as a beam-forming element of a phase array antenna is considered. The phase dynamics of the oscillator array synchronization is used to reshape the phases of signals received from the phase array antenna and improve its beam pattern characteristics.

DOI: 10.1103/PhysRevE.74.056205 PACS number(s): 05.45.Xt

I. INTRODUCTION

The dynamics of arrays of coupled nonlinear oscillators has been a subject of much attention in recent years. This interest is caused by important applications of this model system for understanding the dynamics of coupled Josephson junctions [1], laser arrays [2], etc. Arrays of coupled nonlinear oscillators also can be used as a core technology for phased arrays used as transmitting and receiving antennas in radars and telecommunications [3]. Maintaining certain phase relationships among oscillators (phase synchronization) allows one to control and optimize the directional sensitivity of these antennas ("beam forming"). In Ref. [4], an array of drive-coupled phase oscillators was suggested as a beam-forming element of a transmitter antenna. Recently, arrays of coupled nonlinear oscillators have been proposed as a novel beam-forming element of phase arrays [5,6].

Locally coupled oscillators can be viewed as a discrete analog of the well-known Ginzburg-Landau equation [7]. This system can exhibit a variety of complex spatially nonuniform regimes including wave propagation, spiral turbulence, and chaos. The most interesting phenomenon occurring in a globally coupled array of oscillators with distributed frequencies is the transition to a globally synchronized regime when the coupling strength of oscillators is increased. In the seminal work by Kuramoto (see Ref. [8]) the first analytical theory of synchronization in an array of nonlinear oscillators was developed. This theory is based on a phase approximation which assumes that amplitudes of individual oscillators are slaved to their phases. The magnitude of the mean field found from a self-consistency condition was found to exhibit a second-order phase transition at a certain coupling strength. In subsequent work, a more detailed analysis of this system was performed which also incorporated the effects of external noise and more general coupling among oscillators [9–11]. In Ref. [12] the original Kuramoto model was generalized to allow for variation among coupling coefficients depending on the distance between the units in physical space which allowed one to bridge the gap between the two limiting cases of globally and locally coupled oscillators. In another generalization of the Kuramoto model [13], time delays between coupled units were introduced. In Ref. [14] the Kuramoto model with slowly evolving coupling coefficients was used as a conceptual model of plasticity and learning in networks. There have been a number of studies of the Kuramoto model in external fields (see, for example, [15–17]). In [18,19] the driven dynamics of phase oscillator arrays was studied from the viewpoint of beam forming. Use of synchronization among array of oscillators for the control of the phase distribution along the array with the oscillator natural frequencies were studied in [20,21]. A recent review of the Kuramoto model and its various generalizations can be found in Ref. [22].

In this work we will analyze autonomous and driven dynamics of coupled nonlinear oscillators with *repulsive* coupling [repulsively coupled array (RCA)] which corresponds to the sign reversal of coupling among the oscillators. Section II begins with an illustration of RCA dynamics using numerical simulations of repulsively coupled Stuart-Landau oscillators and then presents our analytical results using the phase oscillator model of the RCA. As we will demonstrate, without driving, an array of oscillators with identical frequencies settles on one of multiple-synchronized regimes characterized by zero mean field. The effects of an external driving of the RCA is discussed in Sec. III. Upon external driving by a periodic signal, the nonzero mean field emerges, and at a finite driving amplitude, all oscillators synchronize with identical phases. The interplay between the phase distribution of the external driving signals and the tendency of oscillators to synchronize provides the phase distribution within the oscillator array which can be beneficial for the array beam forming. The synchronization effects allow one to reduce the level of sidelobes and to make a sharp tip of the main beam. Control and reduction of the sidelobe levels in conventional phase-array antennas can achieved using a spatial windowing applied to the element signals called shading. Section IV discusses application of shading in the nonlinear antenna implemented with the RCA. The results of the study are summarized in Sec. V. A short account of the work on nondriven oscillator arrays with repulsive coupling has been published in Ref. [23].

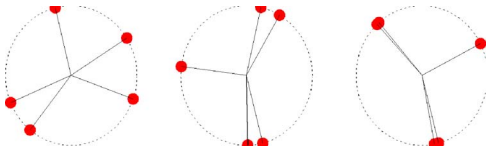

FIG. 1. (Color online) Three possible distributions of individual phases ϕ_j of five oscillators with identical frequencies. All these distributions correspond to the vanishing mean field $R=0$.

II. SYNCHRONIZATION OF STUART-LANDAU OSCILLATORS WITH GLOBAL REPULSIVE COUPLING

In this section we discuss the collective dynamics of repulsively coupled oscillator array without external forcing.

The array of globally coupled Stuart-Landau oscillators is described by equations of the form

$$\dot{z}_j = (G + i\omega_j)z_j - G|z_j|^2 z_j - \frac{\kappa}{N}\sum_{n=1}^{N}(z_n - z_j). \tag{1}$$

Here z_j is a complex variable ($z_j = x_j + iy_j$) describing the state of the jth oscillator, N is the number of oscillators in the array, G is the parameter of nonlinear gain, ω_j is the natural frequency, and κ is the strength of all-to-all coupling. Note the negative sign in front of the coupling term; this choice corresponds to the case of repulsive coupling which is the focus of this paper.

Let us introduce the complex mean field $R(t) = \Sigma_{n=1}^{N} z_n(t)$. For identical natural frequencies of oscillators ($\omega_j = \omega_0$), the mean field reaches zero after an initial transient for arbitrary small negative coupling strength $k < 0$. This stationary regime corresponds to all oscillators having identical amplitudes, but different phases (see Fig. 1). However, the phase distribution has to be neither uniform nor unique: the stationary regime can feature an arbitrary phase distribution ϕ_j among individual oscillators subject to the only constraint $\Sigma_j \exp i\phi_j = 0$.

For unequal frequencies of oscillators, simulations show that the mean field oscillates at small values of coupling. The transition to the synchronized regime depends strongly on the number of oscillators in the array. For two and three oscillators with distributed natural frequencies, the phases of two oscillators synchronize at a certain critical coupling value; however, the mean field R does not turn into zero after the synchronization onset. At larger values of coupling, the mean field gradually approaches zero. For a larger number of oscillators $N > 3$, the oscillators do not synchronize at any value of κ, but the mean field still gradually approaches zero as the strength of repulsive coupling increases.

Phase approximation

For the theoretical analysis of the synchronization dynamics of the RCA we use the standard simplification known as the *phase approximation* (see [19,24]). Namely, we introduce $z_j = a_j e^{i\varphi_j}$ and assume that the magnitudes a_j are slaved to φ_j. This approximation is applicable for $G \gg \kappa$. Furthermore, for large gain G, the amplitudes of all oscillators are close to 1 (see Fig. 2). Ignoring the small deviations $a_j - 1$, we obtain

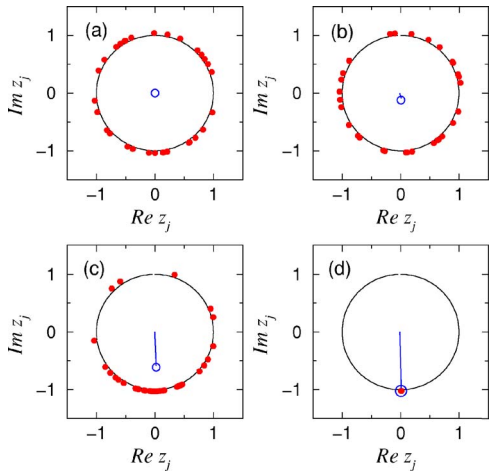

FIG. 2. (Color online) Examples of the oscillator states z_j shown for the array of 32 oscillators for four different values of the amplitude of external driving. (a) $A=0.0$, (b) $A=0.1$, (c) $A=0.5$, and (d) $A=1.0$. The phases of the oscillators (shown by red dots in the complex z plane) rearrange as A increases. The blue open circle marks the value of mean field R. The parameters of simulations are $G=5$, $\tilde{\omega}_j = \omega = 2\pi$, and $\kappa = 0.4$.

the following equation for the phases:

$$\dot{\varphi}_j = \omega_j - N^{-1}\kappa\sum_{n=1}^{N}\sin(\varphi_j - \varphi_n). \tag{2}$$

In this approximation the mean field R (array output) can be written in the form

$$R = re^{i\psi} = \frac{1}{N}\sum_{n=1}^{N} e^{i\varphi_n}, \tag{3}$$

so Eq. (2) becomes

$$\dot{\varphi}_j = \omega_j - \kappa r\sin(\psi - \varphi_j). \tag{4}$$

For N oscillators with identical frequencies $\omega_j = 0$, there exists a family of steady-state solutions of Eq. (2), φ_j^0, corresponding to $r=0$. It can be shown that the Jacobian of the linearized equation (2) reads

$$\mathbf{J} = -\kappa N^{-1}[\mathbf{S}\cdot\mathbf{S}^T + \mathbf{C}\cdot\mathbf{C}^T]$$

and contains a sum of two outer products for vectors $\mathbf{S} = \{\sin\varphi_1^0, \ldots, \sin\varphi_N^0\}^T$ and $\mathbf{C} = \{\cos\varphi_1^0, \ldots, \cos\varphi_N^0\}^T$, respectively. Since the vectors $\mathbf{S}$ and $\mathbf{C}$ are linearly independent, the Jacobian $\mathbf{J}$ has $N-2$ zero eigenvalues and two nonzero eigenvalues. The zero eigenvalues indicate the neutral stability of these trivial solutions with respect to the rearrangement of individual phases. The two nonzero eigenvalues can be found from the equation describing the dynamics of the mean field R,

$$\dot{R} = -\frac{\kappa}{2}\left[R - R^*\frac{1}{N}\sum_{n=1}^{N} e^{2i\varphi_n}\right], \tag{5}$$

which can be obtained by multiplying Eq. (2) by $\exp(i\varphi_j)$ and summing over j. For a slightly perturbed solution corre-

sponding to a small mean field R, one can consider the sum in the last term a complex constant, $C=\frac{1}{N}\Sigma_{j=1}^{N}e^{2i\varphi_j^0}$. The two eigenvalues of Eq. (5) and its complex conjugate are $\lambda_{1,2}=-\frac{\kappa}{2}(1\pm|C|)$. Since $|C|<1$, we obtain that both nonzero eigenvalues are negative.

Therefore, the attractor of the N-dimensional phase space of an array of identical oscillators [2] is an $(N-2)$-dimensional continuous set of neutrally stable steady states. As illustrated in Fig. 1 the final state—i.e., the final distribution of phases—depends on the initial conditions of Eq. (2).

For nonidentical frequencies the dynamics of the array is more complicated and depends on the number of oscillators in the array. We consider here the simple cases of two, three, and many ($N\gg 1$) oscillators.

Case $N=2$. For two oscillators with frequencies $\omega_s\pm\omega_0$, the symmetry dictates that in the synchronized regime the mean field must oscillate at the frequency ω_s and the phases of the oscillators are symmetric with respect to the mean-field phase: $\varphi_1=-\varphi_2=\varphi$. The equation for the single phase φ,

$$\dot{\varphi}=\omega_0+\kappa\cos\varphi\sin\varphi, \tag{6}$$

has two steady-state solutions $\varphi=-\arcsin(2\omega_0\kappa^{-1})/2$ and $\varphi=-\pi/2+\arcsin(2\omega_0\kappa^{-1})/2$ representing synchronized states. It is easy to see that the first solution is unstable, but the second solution is stable. In the synchronized regime ($\kappa>2\omega_0$), the mean field decreases with the coupling strength as

$$R=\sqrt{\frac{1-\sqrt{1-4\omega_0^2/\kappa^2}}{2}}. \tag{7}$$

As the value of $\kappa\omega_0^{-1}$ decreases the stable and unstable synchronized states merge together and disappear when $\kappa\omega_0^{-1}\leqslant 2$, resulting in asynchronous motion with monotonously increasing value of $|\varphi|$.

Case $N=3$. For the case of three oscillators with a symmetric distribution of frequencies $\omega_{1,2,3}=\omega_s,\omega_s\pm\omega_0$, we can introduce the phase differences $\Phi_1=\varphi_2-\varphi_1$ and $\Phi_2=\varphi_1-\varphi_3$. The equations for $\Phi_{1,2}$ read

$$\Phi_1=\omega_0+\frac{\kappa}{3}[\sin(\Phi_1+\Phi_2)-\sin\Phi_2+2\sin\Phi_1],$$

$$\Phi_2=\omega_0+\frac{\kappa}{3}[\sin(\Phi_1+\Phi_2)-\sin\Phi_1+2\sin\Phi_3]. \tag{8}$$

The symmetric synchronized solution corresponds to the fixed point $\Phi_1=\Phi_2=\Phi$ which is defined by the transcendental equation

$$\omega_0=-\frac{\kappa}{3}[\sin\Phi+\sin 2\Phi]. \tag{9}$$

It is easy to see that this equation has two solutions which merge and disappear via a saddle-node bifurcation for

$$\kappa\omega_0^{-1}>\frac{96}{(3+\sqrt{33})\sqrt{30+2\sqrt{33}}}\approx 1.704.$$

However, unlike the case of two oscillators, this condition defines the existence but not the stability of the synchronized solution. To determine the condition for a stable synchronized solution, we linearize Eqs. (8) near the fixed point (9) and obtain the eigenvalues of the system in the following form:

$$\lambda_1=\kappa\cos\Phi,\quad \lambda_2=\frac{\kappa}{3}(2\cos 2\Phi+3\cos\Phi). \tag{10}$$

One can see that both eigenvalues are negative if the steady state Φ is within the range

$$\arccos[(1+\sqrt{33})/8]<|\Phi+\pi|<\pi/2.$$

Therefore, according to Eq. (9) the stability threshold in the case of three oscillators with symmetrically distributed natural frequencies is $k=3\omega_0$.

Now let us turn to the case of many oscillators. We will consider the case of a uniform frequency distribution in the unit interval $[-\omega_0,\omega_0]$; however, the results are qualitatively similar for other distributions as well. In the following we take $\omega_0=1$ since this frequency can be scaled out of the system by changing the time and coupling constant κ. It is easy to see that for large N the synchronized solution must be unstable. Indeed, according to Eq. (4), if there is a completely synchronized solution, the corresponding mean field r must satisfy the condition $kr>1$. Because of the symmetry, this solution has to have a real mean field which we for definiteness assume positive ($\theta=0, r>0$). In the limit of large N the set of equations (4) in the linear approximation decouples, because perturbing the phase of one of the oscillators without changing phases of other oscillators will only affect the mean field by the small amount $O(1/N)$. Therefore, the Lyapunov exponent corresponding to the jth oscillator is $\lambda_j=kr\cos\phi_j+O(1/N)$. At least some of the phases of all oscillators must lie inside the interval $[-\pi/2,\pi/2]$, because otherwise the phase of the mean field was $\theta=\pi$ and not zero. Therefore, at least some of the eigenvalues of the synchronized solution are positive, so the synchronized solution is unstable for arbitrary κ. In fact, our numerical simulations show that the synchronized solution is unstable at any κ for all $N\geqslant 4$.

In the asynchronous regime, the oscillators maintain *on average* their natural frequencies; however, due to coupling, they adjust their phases so as to minimize the mean field. The equation for the mean field, Eq. (5), for nonidentical frequencies can be generalized as

$$\dot{R}=\frac{1}{N}\sum_{n=1}^{N}\omega_n e^{i\varphi_n}-\frac{\kappa}{2}\left[R-R^*\frac{1}{N}\sum_{n=1}^{N}e^{2i\varphi_n}\right]. \tag{11}$$

In the limit of large N the last term on the right-hand side (RHS) can be neglected and the first term can be approximated as $N^{-1}\Sigma_{n=1}^{N}\omega_n e^{i\omega_n t+\xi_n}$, where ξ_n is random phase of individual oscillator. The resultant equation

$$\dot{R} = \frac{1}{N}\sum_{n=1}^{N} \omega_n e^{i\omega_n t+\xi_n} - \frac{\kappa}{2}R \tag{12}$$

can be easily solved. For large κ the mean field can be written as $R=2(\kappa N)^{-1}\Sigma_{n=1}^{N}\omega_n e^{i\omega_n t+\xi_n}$. Taking into account a uniform distribution of natural frequencies $[-\omega_0,\omega]$ one can get the standard deviation of the mean field in the following form:

$$\sigma_r = \frac{2}{\sqrt{3N}}\frac{\omega_0}{\kappa}, \tag{13}$$

which agrees very well with numerical simulations at the large values of N (see Ref. [23]).

III. SYNCHRONIZATION OF THE RCA WITH EXTERNAL PERIODIC SIGNALS

The dynamics of the Kuramoto model driven by external periodic fields has been studied in the literature [15–17,22]. If the frequency of an external field differs from the central frequency of the oscillators, synchronization among the oscillators competes with entrainment to the external signal. For large coupling and small external signal, the mutual synchronization prevails, whereas for large external signal, the mean field synchronizes to the external driving. In this section we consider the case of a driven *repulsively* coupled array whose intrinsic dynamics, as we have seen before, differs qualitatively from that of the classical Kuramoto model. Suppose that all oscillators have identical natural frequencies and each oscillator is driven by a sinusoidal signal $s_j(t)=A\sin(\omega t+\phi_j)$. The array of oscillators is described by the set of driven Stuart-Landau equations

$$\dot{z}_j = (G+i\tilde{\omega}_j)z_j - G|z_j|^2 z_j - \frac{\kappa}{N}\sum_{n=1}^{N}(z_n - z_j) + A\sin(\omega t+\phi_j), \tag{14}$$

where $\tilde{\omega}_j$ now denotes the natural frequency of jth oscillator. We will first consider the case a plane sine wave coming to a linear array of detectors from the broadside direction—i.e., $\phi_j=\phi_0$.

The driving signal induces a sinusoidal mean field in the oscillator array by rearranging the phase distribution among the oscillators; see Fig. 2. At small values of the amplitude A the driving force is insufficient to synchronize the oscillators. However, it modulates the temporal evolution of phases and creates a cluster of temporally phase-locked oscillators which stabilize the phase of the mean field; see Fig. 3. In Fig. 2 the complex amplitude of the mean field R is shown by an open circle in the plane z_j. The amplitude of the mean field is determined by the "compression" of the oscillator phase distribution near within the cluster. Driving at sufficiently large amplitudes A phase-locks the oscillators and forms a δ cluster when all oscillators have identical phases. In this case the synchronization to the driving overcomes the repulsion of phases among the oscillators; see Fig. 2(d).

The magnitude of the mean field, $r=\langle|R(t)|\rangle$, depends on the level of clustering and, therefore, on the amplitude of input signal, A, and the strength of phase repulsion κ. Synchronization of oscillators by the external signal results in the linear input-output characteristics (i.e., r vs A dependence) for $A<A_c$. At $A\geqslant A_c$, the array behaves as a single driven oscillator: the mean-field amplitude saturates and grows slowly with A as a solution of the cubic equation $r-r^3=A/G$. These features are illustrated by a three-dimensional (3D) plot of r as a function of A and κ; see Fig. 4. The plot shows that as the repulsive forces increase, with larger values of κ, a larger amplitude of driving is required to overcome the repulsion and form a point cluster.

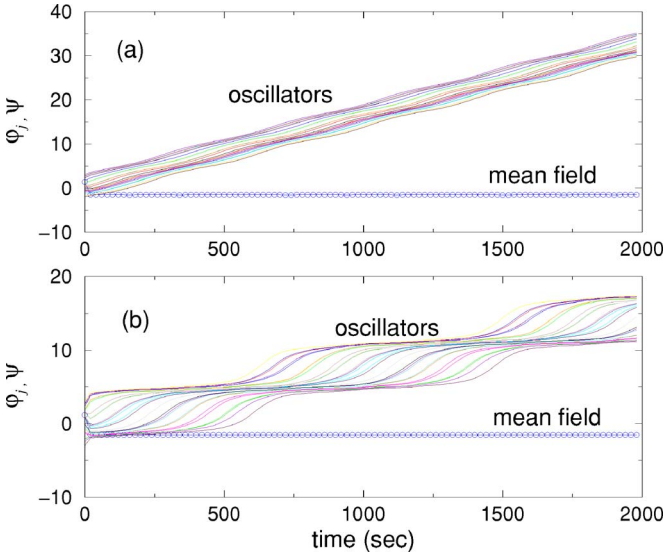

FIG. 3. (Color online) Time evolution of the oscillator phases φ_j and the mean-field phase ϕ for (a) $A=0.1$ and (b) $A=0.5$. The parameters of simulations are $N=32$, $G=5$, $\tilde{\omega}_j=\omega=2\pi$, and $\kappa=0.4$. Despite the slow drift of the oscillator phases the phase of mean field remains steady.

As follows from the synchronization theory, the threshold value A_c for the onset of synchronization depends on the frequency mismatch of ω and ω_j. This threshold vanishes only the case of $\omega=\omega_j$ which is considered above. When $\omega\neq\omega_j$, beats in the individual oscillators precede the onset of complete synchronization. Due to clustering, these beats average down in the mean field and decrease its amplitude r.

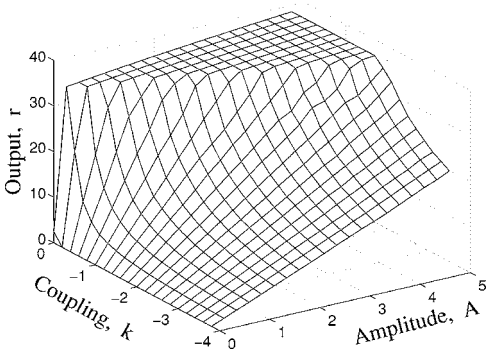

FIG. 4. The dependence of RCA output on the coupling strength κ and the amplitude A of the driving signal for $N=32$, $G=5$, and $\tilde{\omega}_j=\omega=2\pi$.

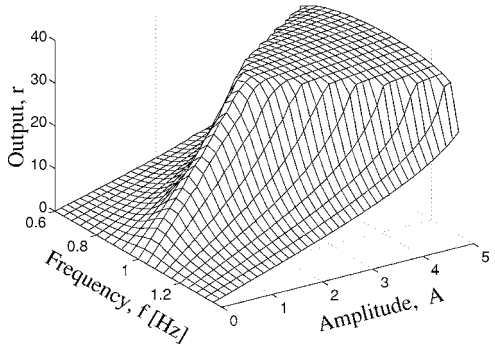

FIG. 5. The dependence of RCA output on the frequency of received signal $f=\omega/2\pi$ for $N=32$, $G=5$, $\tilde{\omega}_j=2\pi$, and $\kappa=1$

The occurrence of beats also results in the nonlinearity of input-output characteristics; see Fig. 5.

A. Phase approximation

This approximation is applicable for $G \gg \kappa, A$. Furthermore, for large gain G, the amplitudes of all oscillators are close to one (see Fig. 2). Ignoring the small deviations $a_j - 1$, we obtain the following equation for the phases:

$$\dot{\varphi}_j = \tilde{\omega}_j - \frac{\kappa}{N}\sum_{n=1}^{N} \sin(\varphi_n - \varphi_j) + A \sin(\phi_j - \varphi_j) + \xi_j, \quad (15)$$

where $\omega_j = \tilde{\omega}_j - \omega$. Here we also added white zero-mean Gaussian noise acting independently on all oscillators, $\langle \xi_j(t) \rangle = 0, \langle \xi_j(t) \xi_k(t') \rangle = 2D\delta(t-t')\delta_{jk}$.

In this approximation the mean field R (array output) can be written in the form (3), so Eq. (15) becomes

$$\dot{\varphi}_j = \omega_j - \kappa r \sin(\psi - \varphi_j) + A \sin(\phi_j - \varphi_j) + \xi_j. \quad (16)$$

For large N, the mean field R is not fluctuating and becomes a deterministic function. Then we can introduce the single-oscillator probability distribution function $W_j(\varphi, t) \equiv W(\varphi, t; \omega_j, \phi_j) = \langle \varphi - \varphi_j(t) \rangle$ and write a Fokker-Planck equation for $W_j(\varphi, t)$:

$$\frac{\partial W_j}{\partial t} = -\frac{\partial}{\partial \varphi}[F_j(\varphi) W_j] + D\frac{\partial^2 W}{\partial \varphi^2}, \quad (17)$$

where the "phase drift velocity" $F_j(\varphi) = \omega_j - \kappa r \sin(\psi - \varphi) + A \sin(\phi_j - \varphi)$ is a 2π-periodic function of φ (a similar equation for the case of nondriven noisy oscillators was derived in Refs. [25,26] and then often used in bifurcation analyses; see [22] for a review).

The stationary solution of Eq. (17) satisfying the periodic boundary condition $W_j(\varphi) = W_j(\varphi + 2\pi)$ is given by (cf. [9,27])

$$W_j(\varphi) = W_j(0) \exp\left(\frac{\omega_j \varphi + A \cos(\varphi - \phi_j) - \kappa r \cos(\varphi - \psi) + \kappa r \cos\psi - A \cos\phi_j}{D} \right) \times \left\{ 1 + \frac{(e^{-2\pi\omega_j/D} - 1) \int_0^{\varphi} e^{[-\omega_j \tilde{\varphi} + \kappa r \cos(\tilde{\varphi} - \psi) - A\cos(\phi_j - \tilde{\varphi})]/D} d\tilde{\varphi}}{\int_0^{2\pi} e^{[-\omega_j \tilde{\varphi} + \kappa r \cos(\tilde{\varphi} - \psi) - A\cos(\phi_j - \tilde{\varphi})]/D} d\tilde{\varphi}} \right\}, \quad (18)$$

where $W_j(0)$ is determined by the normalization condition

$$\int_0^{2\pi} W_j(\varphi) d\varphi = 1. \quad (19)$$

The mean field R can be calculated as

$$R = \frac{1}{N}\sum_{n=1}^{N} \int W_n(\varphi) e^{i\varphi} d\varphi. \quad (20)$$

For large N we can replace the sum by the integration over the frequency and driving phase (ϕ) distributions,

$$R = \int_{-\infty}^{\infty} g(\omega) d\omega \int_0^{2\pi} H(\phi) d\phi \int_0^{2\pi} d\varphi W(\varphi; \omega, \phi) e^{i\varphi}. \quad (21)$$

This complex integral equation has to be solved to obtain R.

To simplify the problem, we first neglect the noise, $D=0$. Then the stationary solution of the Fokker-Planck equation is much simpler,

$$W_j(\varphi) = \frac{V_i}{\omega_j - \kappa r \sin(\psi - \varphi) + A \sin(\phi_j - \varphi)}, \quad (22)$$

where

$$V_i = \left[\int_0^{2\pi} d\phi [\omega_j - \kappa r \sin(\psi - \varphi) + A \sin(\phi_j - \varphi)]^{-1} \right]^{-1}$$

is the normalization constant.

Additional simplification is achieved if one neglects the frequency spread $[g(\omega) = \delta(\omega - \omega_0)]$ and considers the broadside direction signal $[H(\phi) = \delta(\phi)]$. Then the probability distributions for all oscillators are identical and the self-consistency equation can be written in the form

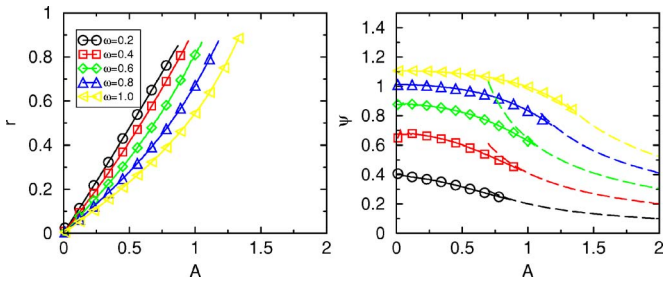

FIG. 6. (Color online) The dependence of the mean-field amplitude r (left panel) and phase ψ (right panel) on the magnitude of the incoming signal for several values of the driving frequency detuning ω_0 for repulsive coupling $\kappa=1$. Dashed lines show the phase of the mean field for the completely synchronized regime.

$$re^{i\psi} = \int_0^{2\pi} \frac{e^{i\varphi} d\varphi}{F(\varphi)} \left[\int_0^{2\pi} \frac{d\varphi}{F(\varphi)} \right]^{-1}, \tag{23}$$

where $F(\varphi)=\omega_0-\kappa r \sin(\psi-\varphi)-A \sin \varphi$.

A solution of Eq. (23) can be found numerically by the method of iterations: we take initial guess values of r_0, ψ_0 on the RHS of Eq. (23), perform the integration, and obtain the next iteration values r_1, ψ_1. Then we substitute them into the RHS again and so on. The iteration process quickly converges to the correct values of r and ψ. Figure 6 shows the dependences $r(A)$ and $\psi(A)$ obtained using this method. As seen from the plots, the theoretical dependences are in good agreement with the numerical data, Figs. 4 and 5.

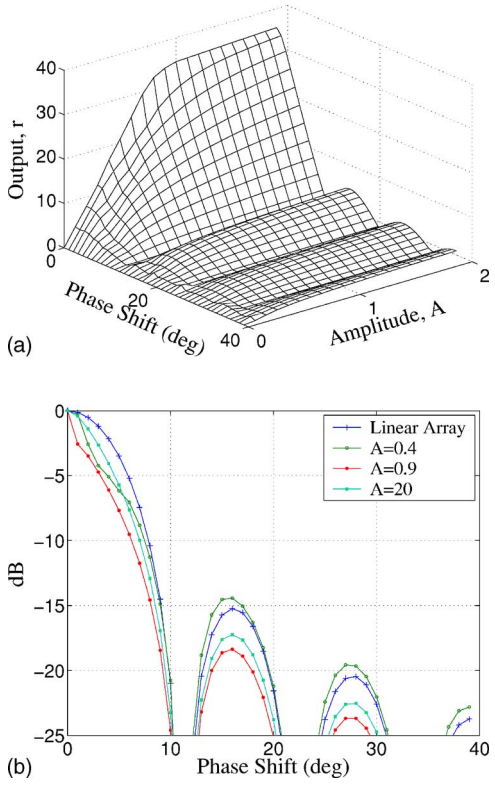

FIG. 7. (Color online) The dependence of beam pattern on the amplitude of the received signal A for $N=32$, $G=5$, $\tilde{\omega}_j=\omega=2\pi$, and $\kappa=0.4$. 3D plot of the dependence (top panel) and the comparison of the selected beam patters in NLBF with linear BF (bottom panel).

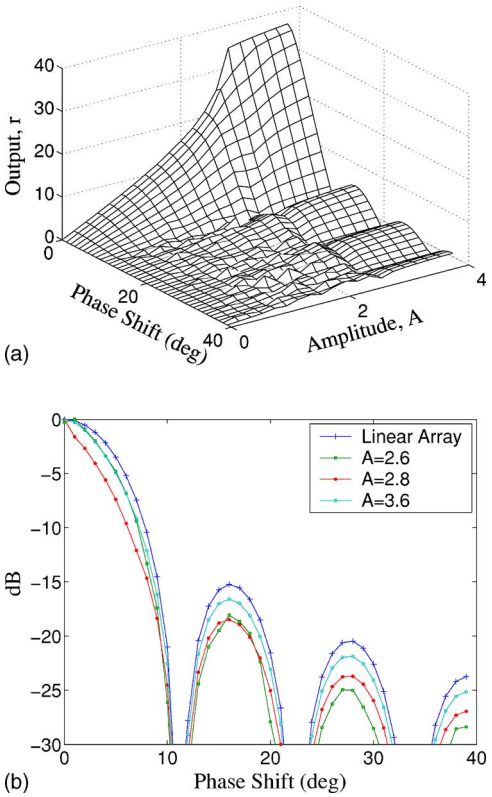

FIG. 8. (Color online) The dependence of beam pattern on the amplitude of the received signal A with frequency $\omega=2.4\pi$. $N=32$, $G=5$, $\tilde{\omega}_j=2\pi$, and $\kappa=0.4$. 3D plot of the dependence (top panel) and the comparison of the selected beam patters in NLBF with linear BF (bottom panel).

For small ω_0, the solution approaches $r=A/\kappa$, $\psi=0$ for $A<\kappa$, and $r=1$ for $A>\kappa$. It is easy to see that $r=-A/\kappa$, $\psi=0$ is the solution of $F(\varphi;r,\psi)=0$ for $\omega=0$. This solution corresponds to an arbitrary probability distribution satisfying the condition $\int W(\varphi)d\varphi=r$. At $A\to\kappa$, the probability distribution approaches $\delta(\varphi)$; i.e., all oscillators become synchronized with identical phases.

For arbitrary ω_0, at a certain threshold value of A the amplitude of the mean field becomes 1, which indicates that all oscillators acquire identical phases equal to the mean-field phase ψ. Thus, one can find the phase of the mean field in the totally synchronized regime as $\psi=-\arcsin(\omega_0/A)$.

B. Beam-forming performance of the RCA

Here we consider a generalization of the model (15) to allow signals with different phases acting on different oscillators. In the simplest case, it may correspond to a sinusoidal signal arriving at a linear oscillator array at a certain angle Θ with respect to the broadside direction; then, the jth oscillator receives a signal $s_j=A \sin(\omega t+\phi_j)$. The phases of the signals at nearby elements are related as $\phi_j=\phi_{j-1}+\Delta$, where the phase shift depends on the angle Θ, wavelength λ, and dis-

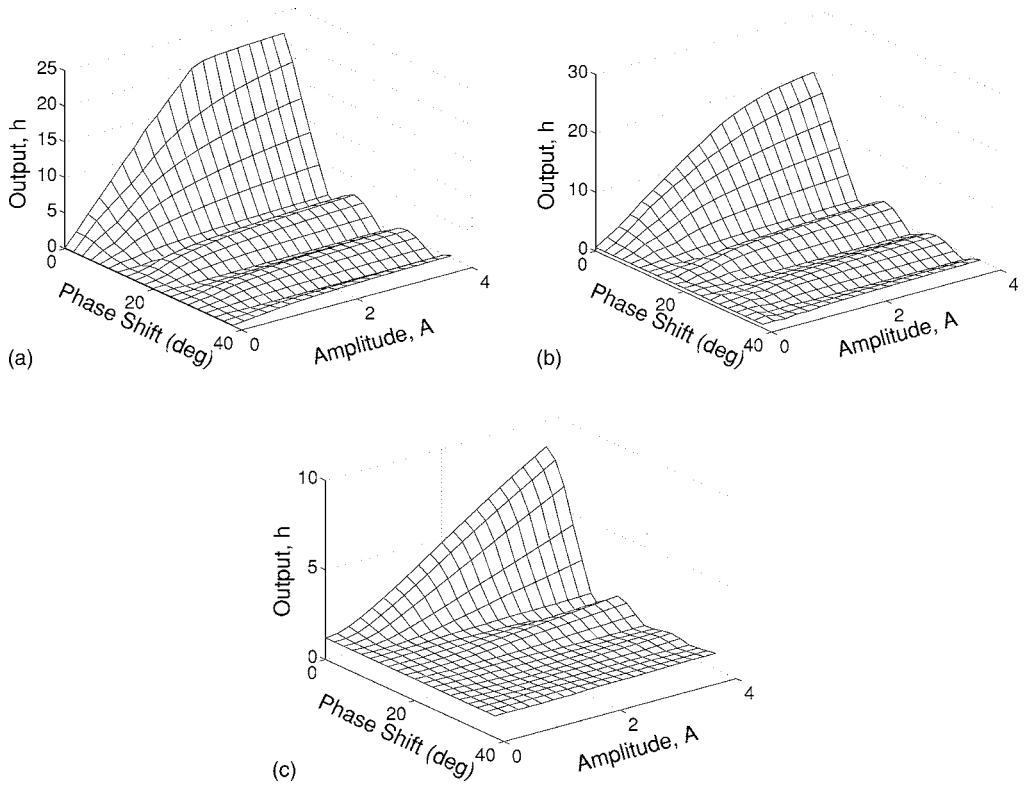

FIG. 9. The dependence of beam pattern on the amplitude of the received signal A for different levels of noise: $\sigma=1.0$ (a), $\sigma=5.0$ (b), and $\sigma=20.0$ (c). Parameters $N=32$, $G=5$, $\tilde{\omega}_j=\omega=2\pi$, and $\kappa=0.4$.

tance between the elements d, $\Delta=360^\circ\frac{d}{\lambda}\cos\Theta$. Such signals synchronize the array of oscillators and form a specific distribution of phases along the array. Due to repulsive forces between the oscillators, their phases will differ from the phases of the received signals. The oscillator array will tend to spread these phases. This provides a dynamical mechanism behind the improvement of beam pattern characteristics in this nonlinear beam former (NLBF).

The beam patterns computed in a chain of 32 nonlinear oscillators are shown in Fig. 7. The 3D plot of the array output, r, as function of phase shift Δ and signal amplitude shows that the shape of the beam patterns changes with the amplitude. There exist an optimal value of A in terms of beam pattern characteristics. At this value of A the main lobe has the most sharp tip in the broadside direction and the maxima of sidelobes of the normalized beam pattern are reduced to the lowest levels; see Fig. 7(b) (red curve). Our simulations with various parameter settings indicate that such optimal values of A occur at the threshold where the gain of the array start experiences saturation when the phase array is turned to the direction of the signal source.

In the case when $\omega\neq\omega_j$ the synchronization of the array is characterized by the nonlinear dependence of output r on the values of input amplitude A; see Fig. 8. The optimal values of A also increase. The main beam in the NLBF sharper and the side lobes are 3–4 dB lower than for a conventional beam former; see Fig. 8 (right panel).

C. Synchronization to a noisy signal

Due to the lack of superposition in the nonlinear oscillator array, noise in the received signal will alter the behavior of

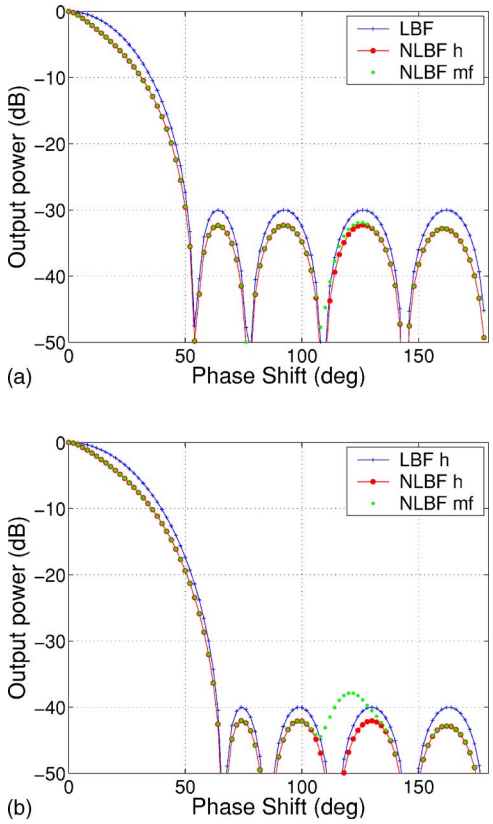

FIG. 10. (Color online) Normalized beam patterns for $N=10$, $\kappa=0.4$, and $\omega=\tilde{\omega}_j=2\pi$ obtained using Chebyshev windows with 30 dB and 40 dB sidelobe ratio.

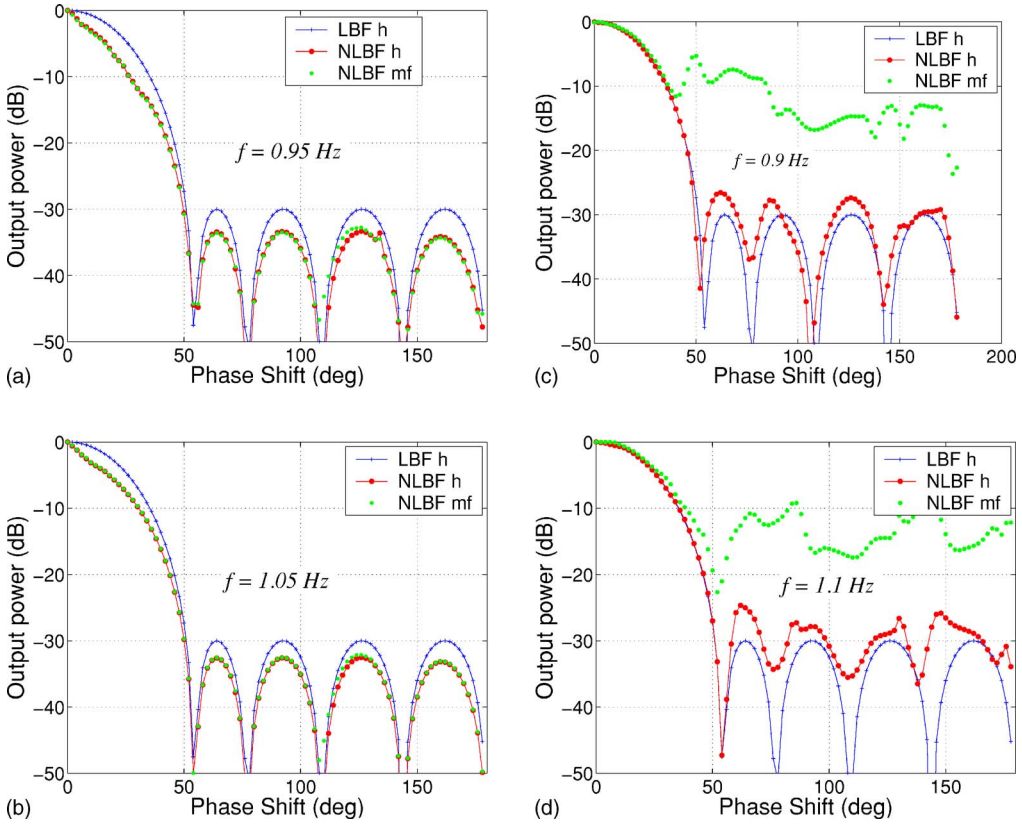

FIG. 11. (Color online) Normalized beam patterns for $N=10$, $\kappa=0.4$, and $\tilde{\omega}_j=2\pi$ obtained using a Chebyshev window with 30 dB sidelobe ratio and four different values of driving frequency.

the NLBF. To explore these changes we simulated the array of oscillators that receives a sinusoidal plane wave of amplitude A and white Gaussian noise with standard deviation σ. The noise signals acting on different oscillators were uncorrelated. Beam patterns in these simulations were plotted using power spectrum analysis of the output mean field $\Sigma_{n=1}^{N} z_n$. The power spectrum distribution was computed using Hanning window for 1024 samples generated with 50 samples/sec and averaged 5 times. Harmonic h occurred in the spectrum of the mean field at the frequency of the sinusoidal source signal was treated as the output signal NLBF. The beam pattern computed for the amplitude of the harmonic h is shown in Fig. 9.

The simulations show that additional noise decreases the NLBF gain. As a result the optimal values of amplitude A increase; compare Figs. 9(a)–9(c). The decrease of the gain can be explained by the influence of noise on the quality of synchronization. The noise tends to reduce the synchrony in the array by spreading the cluster of phases. As a result higher values of the external synchronizing signal are needed to form the cluster.

IV. SHADING FOR THE NLBF

The results presented above show that the use of synchronizing oscillators in phase array antennas allows one to reduce the levels of sidelobes by 2–4 dB. However, in the theory of conventional (linear) arrays there are techniques of beam pattern synthesis that allow one to reduce sidelobes to much lower levels at the expense of the main beamwidth. This is done by applying appropriate windowing to the array signals, which is known as shading. A popular approach to forming amplitude tapers is the Dolph-Chebyshev technique which gives the narrowest possible main lobe for a given maximum sidelobe level [28–30].

In order to apply shading to the array of oscillators we rewrite Eq. (1) in the following form:

$$\dot{z}_j = (G + i\omega_j)z_j - G|z_j|^2 z_j + \kappa[R(t) - z_j] + s_j(t), \qquad (24)$$

where the complex "shaded" mean field

$$R(t) = \frac{1}{N}\sum_{n=1}^{N} w_n z_n(t) \qquad (25)$$

replaces the standard mean field $R(t)$ used earlier. Here w_n are weights used for the shading. The modified mean field (25) is also used as the output signal of the NLBF. The weights w_n can be computed using the MatLab function chebwin (N,Q), where N is the number of elements and Q is the difference between magnitudes of sidelobes and the main beam in dB.

Here we present the results obtained for a line array of ten elements. To evaluate how shading affects the beam patterns we apply the input signal $s_j(t)=A\sin(\omega t+j\Delta)$ to each oscillator and compute the amplitude of the mean field, $r=\langle|R(t)|\rangle$, and the amplitude of the harmonic at the frequency

ω measured in the power spectrum of Im $R(t)$. The beam patterns plotted for these amplitudes are denoted "NLBF mf" and "NLBF h," respectively. The results are compared with the harmonic amplitude in the power spectrum of the output signal in the standard linear beam former "LBF h" computed with the same shading coefficients. We use the parameters of the array, $\kappa=0.4$, $G=5$, and $\omega_j=2\pi$, and the amplitude of input signals is set close to the optimal value of the NLBF, $A=0.9$.

Figure 10 shows the beam patterns obtained with Chebyshev coefficients evaluated for the cases of $Q=30$ dB (top) and $Q=40$ dB (bottom). In the first case the values of the mean field and the harmonic amplitudes are close to each other for all values of the phase shift Δ. This is indicative of the synchronization between the oscillators and the input signal. In the second case the synchronization apparently becomes unstable within the range of Δ from 110° to 130° where beats in the mean field occur. Comparison of NLBF h with LBF h shows that sidelobes in the nonlinear beam former are about −2.5 dB lower than in the standard shaded array. This effect is mostly due to the reshaping (sharpening) of the main beam and the normalization of the beam patterns to their maximum values.

The beam patterns presented in Fig. 11 show how the frequency mismatch between ω and $\omega_j=2\pi$ influences the shading effect and synchronization of the oscillators. The two top panels present the beam patterns for the cases when the frequency mismatch is relatively small (about 5%) and synchrony to the input signal is preserved. When the frequency mismatch increases beyond the synchronization thresholds the effect of shading in the oscillator array deteriorates rapidly. The destruction of synchronization between the signal and oscillators can be easily seen in the behavior of the mean field "NLBF mf." Therefore, the shading technique can improve the beam pattern of NLBF only when the frequencies of the oscillators are close to the frequency of the source signal.

The effect of noise on the shading quality is illustrated by Fig. 12 which shows shaded beam patterns for two values of the standard variance σ of the white Gaussian noise added to the sinusoidal input signal. For small levels of noise the NLBF provides an improvement over the standard beam former (LBF); see Fig. 12 (top). However, with an increase of noise to moderate levels this effect decreases Fig. 12 (bottom).

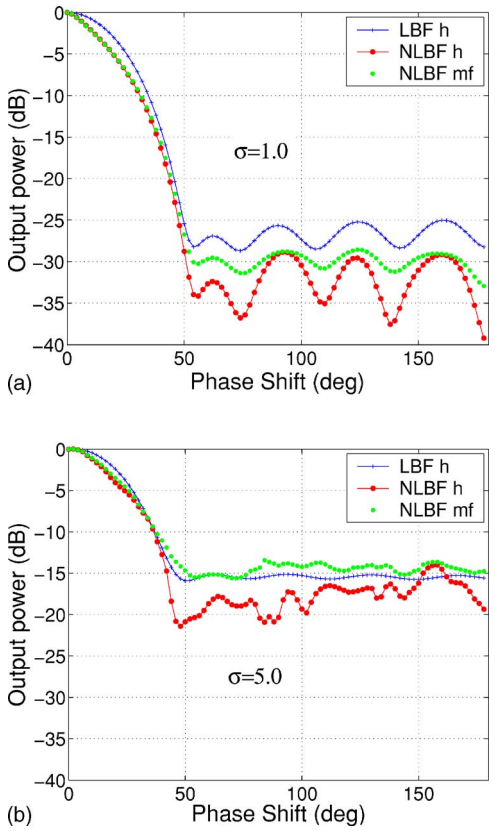

FIG. 12. (Color online) Normalized beam patterns for $N=10$, $G=5$, $\kappa=0.4$, and $\omega=\tilde{\omega}_j=2\pi$ obtained using a Chebyshev window with 30 dB sidelobe ratio in the case of additive noise.

V. CONCLUSION

In this paper we considered the dynamics of repulsively coupled Stuart-Landau oscillators in the autonomous regime as well as under the influence of external periodic signal. Without external driving, this system quickly converges to a regime which minimizes the mean field. For identical oscillators, the mean field turns into zero for any nonzero coupling coefficient, whereas for nonidentical frequencies, the mean field remains finite at any finite value of the coupling. Furthermore, for the number of oscillators $N>3$, the repulsive coupling fails to synchronize the array and the mean field remains fluctuating for any value of the coupling constant. In case of a driven array, the mean field remains nonzero even for identical oscillators. We found the amplitude of the mean field as a function of external driving and frequency detuning analytically using a phase approximation and solving the self-consistency equation.

Using a line array of globally coupled identical oscillators as a model for a phase array receiving antenna we studied the effect of repulsive coupling of the formation of beam patterns. The sinusoidal signal received from the broadside direction of the array can synchronize the array oscillators in a uniform state of the phase distribution. The threshold amplitude of the signal required for such a synchronization is proportional to the strength of the repulsive coupling among the oscillators. When the signal source is moved out of the broadside direction the input signals have different phases at the inputs of the oscillators. In this case repulsive coupling alters the original distribution of the phases in the synchronized array toward reduced values of the mean-field amplitude—i.e., spreading the oscillators phases. This nonlinear mechanism results in a change of the beam pattern. The tip of the main beam becomes sharper and the levels of sidelobes are reduced. The effect is larger when the oscillators are near the threshold where synchronization to the signal overcomes the repulsive forces.

[1] K. Wiesenfeld, P. Colet, and S. H. Strogatz, Phys. Rev. E **57**, 1563 (1998).
[2] M. Silber, L. Fabiny, and K. Wiesenfeld, J. Opt. Soc. Am. B **10**, 1121 (1993).
[3] R. Tang and R. W. Burns, in *Antenna Engineering Handbook*, 3rd ed., edited by R. C. Johnson (McGraw-Hill, New York, 1993).
[4] T. Heath, K. Wiesenfeld, and R. A. York, Int. J. Bifurcation Chaos Appl. Sci. Eng. **10**, 2619 (2000).
[5] M. Gabbay and M. L. Larsen (unpublished).
[6] M. Gabbay, M. L. Larsen, and L. S. Tsimring, Phys. Rev. E **70**, 066212 (2004).
[7] I. S. Aranson and L. Kramer, Rev. Mod. Phys. **74**, 99 (2002).
[8] Y. Kuramoto, *Chemical Oscillations, Waves, and Turbulence* (Springer, Berlin, 1991).
[9] H. Sakaguchi, Prog. Theor. Phys. **79**, 39 (1988).
[10] J. D. Crawford, Phys. Rev. Lett. **74**, 4341 (1995)
[11] S. H. Strogatz, Physica D **143**, 1 (2000)
[12] P.-J. Kim, T.-W. Ko, H. Jeong, and H.-T. Moon, Phys. Rev. E **70**, 065201(R) (2004).
[13] M. K. Stephen Yeung and S. H. Strogatz, Phys. Rev. Lett. **82**, 648 (1999).
[14] P. Seliger, S. C. Young, and L. S. Tsimring, Phys. Rev. E **65**, 041906 (2002).
[15] S. Shinomoto and Y. Kuramoto, Prog. Theor. Phys. **75**, 1105 (1986).
[16] H. Sakaguchi, S. Shinomoto, and Y. Kuramoto, Prog. Theor. Phys. **79**, 1069 (1988).
[17] J. A. Acebrón and L. L. Bonilla, Physica D **114**, 296 (1998).
[18] B. K Meadows, T. H. Heath, J. D. Neff, E. A. Brown, D. W. Fogliatti, M. Gabbay, V. In, P. Hasler, S. P. DeWeerth, and W. L. Ditto, Proc. IEEE **90**, 882 (2002).
[19] M. Gabbay, M. L. Larsen, and L. S. Tsimring, Proc. SPIE **5559**, 146 (2004).
[20] A. A. Dvornikov, G. M. Utkin, and A. M. Chukov, Radiotekh. Elektron. (Moscow) **24**, 2254 (1979) [Radio Eng. Electron. Phys. **24**, 76 (1979)].
[21] A. A. Dvornikov, G. M. Utkin, and A. M. Chukov, Radiofiz. **27**, 1384 (1984) [Radiophys. Quantum Electron. **27**, 967 (1984)].
[22] J. A. Acebrón *et al.*, Rev. Mod. Phys. **77**, 137 (2005).
[23] L. S. Tsimring, N. F. Rulkov, M. L. Larsen, and M. Gabbay, Phys. Rev. Lett. **95**, 014101 (2005).
[24] P. S. Hagan, SIAM J. Appl. Math. **42**, 762 (1982).
[25] L. L. Bonilla, J. Stat. Phys. **659**, 46 (1987).
[26] S. H. Strogatz and R. E. Mirollo, J. Stat. Phys. **63**, 613 (1991).
[27] R. L. Stratonovich, *Topics in the Theory of Random Noises* (Gordon and Breach, New York, 1967).
[28] C. L. Dolph, Proc. IRE **34**, 335 (1946).
[29] J. D. Kraus, *Antennas*, 2d ed. (McGraw-Hill, New York, 1988).
[30] P. Lynch, Mon. Weather Rev. **125**, 655 (1997).